Platinum Metal Complexes of Potentially Chelating Alkene Thioether and Selenoether Ligands: The Synthesis and Dynamic Nuclear Magnetic Resonance Study of $[MX_2\{E[(CH_2)_nCR{=}CR_2]_2\}]$ (M = Pt or Pd; X = Cl, Br, or I; E = S or Se; n = 2 or 3; R = H or Me) and the *X*-Ray Crystal Structure of *cis*-Di-iodo-(5-thianona-1,8-diene)platinum(II), $[PtI_2\{S[(CH_2)_2CH{=}CH_2]_2\}]$†

Edward W. Abel, David G. Evans,* Julian R. Koe, and Vladimir Sik
Department of Chemistry, University of Exeter, Exeter EX4 4QD
Michael B. Hursthouse and Paul A. Bates
Department of Chemistry, Queen Mary College, London E1 4NS

A variety of potentially tridentate dialkenyl chalcogenide ligands have been found to act as bidentate ligands in platinum(II) halide complexes. The complexes undergo a very facile fluxional process whereby the pendant, unco-ordinated alkene moiety displaces the co-ordinated alkene moiety. Inversion of configuration at the pyramidal chalcogen atom is also observed and the energy barrier for this is typical of dihalogeno-platinum(II) chalcogenide complexes and much greater than the energy barrier for the alkene-replacement process. The molecular structure of a representative species, $[PtI_2\{S[(CH_2)_2CH{=}CH_2]_2\}]$, has been determined. The crystals are monoclinic with space group $P2_1/n$ with Z = 4 in a unit cell of dimensions a = 13.249(3), b = 8.804(3), c = 11.656(3) Å, and β = 101.05(2)°. The pendant chain is positioned at maximum displacement from the co-ordination sphere of the metal.

In this paper we report the synthesis of some dialkenyl chalcogenide complexes of *cis*-dihalogeno-platinum(II) and -palladium(II) and a study of their structural and fluxional properties. In these complexes the metal atom is situated at the centre of the square plane composed of the two *cis*-halide ions, the chalcogen atom, and the centroid of the co-ordinated alkene moiety. The other alkenyl chain is pendant with an unco-ordinated C=C double bond.

Hitherto, the study of the chemistry and stereochemistry of the complexes most closely related to those reported here has involved either those with monoalkenyl chalcogenide ligands[1-3] or those with alkenylphosphine ligands.[4,5] In the monoalkenyl chalcogenide complexes the fluxional process of chalcogen inversion has been observed[6,7] and in the alkenylphosphine complexes where there are at least two alkenyl groups the alkene groups have been observed to replace each other at the co-ordination sites in another fluxional process.

Results and Discussion

Preparation and Properties of the Complexes.—The dialkenyl chalcogenide ligands were prepared using a two-phase liquid system with a phase-transfer catalyst and reacted readily in equimolar proportions with potassium tetrachloroplatinate(II) or sodium tetrachloropalladate(II) at room temperature, in aqueous ethanolic solution left stirring overnight, to form the chloro complexes discussed below. The corresponding bromo and iodo complexes were readily prepared by metathesis in warm acetone solution.

The nature of the product formed depends very much on the length of the alkenyl chain in the ligands, which are all of the general type $E[(CH_2)_nCR^1{=}CR^2R^3]_2$, L^1—L^6. When n = 2, the products were all isolated as crystalline solids, soluble in common solvents and fully characterised on the basis of analytical and spectroscopic data. The products all have the stoicheiometry $[MX_2(L)]$ (M = Pt or Pd; X = Cl, Br, or I; L = L^1, L^2, L^4, or L^6) and the solid-state structure shown in

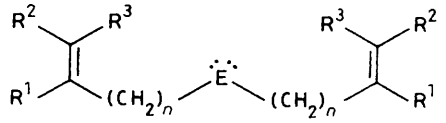

L^1 E = S, R^1 = R^2 = R^3 = H, n = 2
L^2 E = Se, R^1 = R^2 = R^3 = H, n = 2
L^3 E = S, R^1 = R^2 = R^3 = H, n = 3
L^4 E = S, R^1 = H, R^2 = R^3 = Me, n = 2
L^5 E = S, R^1 = Me, R^2 = R^3 = H, n = 1
L^6 E = S, R^1 = Me, R^2 = R^3 = H, n = 2

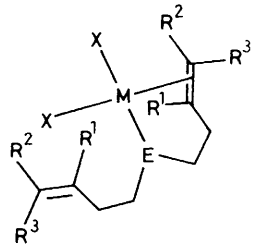

(A) M = Pt; X = Cl, Br, or I; E = S or Se, R^1R^2, R^3 = H or Me

(A). For the case of the longer alkenyl chain L^3 where n = 3, E = S, and R^1 = R^2 = R^3 = H, the product formed on reaction of the ligand is a yellow oil which could not be crystallised despite repeated attempts and which did not survive column chromatography (Florisil). The oil did however give a ^{1}H n.m.r. spectrum similar to those obtained for the complexes of L^1 and L^2, consistent with its formulation as $[PtCl_2L^3]$. For

† *Supplementary data available:* see Instructions for Authors, *J. Chem. Soc., Dalton Trans.*, 1989, Issue 1, pp. xvii—xx.

the shortest alkenyl chain L^5 with $n = 1$, E = S, R^1 = Me, and $R^2 = R^3 = H$ the only product which could be isolated was shown to be the bis(thioether) complex $[PtCl_2L^5_2]$ on the basis of elemental analysis and spectroscopic evidence, indicating that formation of a small strained ring is unfavourable.

Infrared data and elemental analyses for all the new compounds are reported in Tables 1 and 2 respectively. In order to assign the stereochemistry of the complexes however a single-crystal *X*-ray structure was required and the results for one member of the series, $[PtI_2L^1]$, are discussed in the following section.

Crystal and Molecular Structure of cis-*Di-iodo(5-thianona-1,8-diene)platinum*(II), $[PtI_2L^1]$.—The molecular structure of $[PtI_2L^1]$ determined from the *X*-ray crystallographic analysis is shown in Figure 1 and selected intramolecular bond lengths and angles are given in Table 3. The fractional atomic co-ordinates are given in Table 4.

The complex is essentially square planar in the solid state with respect to the *cis*-iodine atoms, the co-ordinated alkene centroid, and the sulphur atom, with the platinum atom situated in the centre. In this respect the structure is similar to that of *cis*-dibromo(6-thiahept-1-ene)platinum(II), $[PtBr_2L^7]$.[3] The two structures differ, however, in the configuration at the sulphur atom. In *cis*-dibromo(6-thiahept-1-ene)platinum(II) the configuration at sulphur is pseudo-equatorial with respect to the plane, whereas in $[PtI_2L^1]$ it is pseudo-axial. This is presumably so that the larger unco-ordinated alkenyl group in the latter complex may place the unco-ordinated alkene moiety at the greatest possible distance from the chalcogen atom in the least sterically congested configuration. It may be conjectured that another reason for this configuration also exists: in the non-rigid state a pseudo-axial orientation at sulphur allows the bending of the pendant alkenyl chain to position the unco-ordinated alkene moiety directly above the site of the co-ordinated alkene moiety. This point is discussed in the n.m.r. section (see below).

The co-ordinated alkene centroid to platinum bond in $[PtI_2L^1]$ has a length of 2.086 Å and is close to that observed in $[PtBr_2L^7]$ (2.047 Å), the small difference being due to a balance between the opposing factors of a smaller ring size and a greater halogen *trans* influence in the dialkenyl sulphide complex. These values are consistent with those observed in other platinum(II)–alkene complexes, *e.g.* in Zeise's salt[8] the alkene centroid–platinum distance is 2.014 Å and in *trans*-dichloro(dimethylamine)(ethene)platinum(II)[9] it is 2.09 Å. The platinum–sulphur bond length of 2.280(5) Å is typical of that observed in other similar compounds, *e.g.* in *cis*-dibromo(6-thiahept-1-ene)platinum(II)[3] the Pt–S bond length is 2.286 Å and in *cis*-$[PtCl_2\{S(Me)CH_2CH_2CH(CO_2H)NH_2\}]$[10] it is 2.26 Å.

Table 1. I.r data (cm^{-1})

Sample	Sample state	Alkene stretch: co-ordinated	Alkene stretch: unco-ordinated
L^1	Liquid film	—	1 642
L^3	Liquid film	—	1 641
L^5	Liquid film	—	1 648
L^4	Liquid film	—	*
L^6	Liquid film	—	1 650
L^2	Liquid film	—	1 640
$[PtCl_2L^1]$	KBr disc	1 502	1 642
$[PtBr_2L^1]$	KBr disc	1 500	1 641
$[PtI_2L^1]$	KBr disc	1 496	1 640
$[PtCl_2L^5_2]$	KBr disc	—	1 644
$[PtCl_2L^4]$	KBr disc	1 501	*
$[PtCl_2L^2]$	KBr disc	1 508	1 641
$[PtBr_2L^2]$	KBr disc	1 504	1 641
$[PtI_2L^2]$	KBr disc	1 500	1 639
$[PdCl_2L^5_2]$	KBr disc	—	1 645
$[PtCl_2L^6]$	KBr disc	1 515	1 650
$[PtBr_2L^6]$	KBr disc	1 514	1 650
$[PtI_2L^6]$	KBr disc	1 512	1 647

* Band expected not observed.

Table 3. Bond lengths (Å) and angles (°) for $[PtI_2L^1]$

I(1)–Pt	2.613(4)	I(2)–Pt	2.593(4)
S–Pt	2.280(5)	C(3)–Pt	2.221(13)
C(4)–Pt	2.178(12)	C(1)–S	1.829(13)
C(5)–S	1.829(14)	C(2)–C(1)	1.505(19)
C(3)–C(2)	1.533(20)	C(4)–C(3)	1.395(20)
C(6)–C(5)	1.537(20)	C(7)–C(6)	1.511(25)
C(8)–C(7)	1.208(28)		
I(2)–Pt–I(1)	91.2(1)	S–Pt–I(1)	174.1(1)
S–Pt–I(2)	87.3(2)	C(3)–Pt–I(1)	94.5(5)
C(3)–Pt–I(2)	162.1(4)	C(3)–Pt–S	85.4(5)
C(4)–Pt–I(1)	90.1(5)	C(4)–Pt–I(2)	160.3(4)
C(4)–Pt–S	93.3(5)	C(4)–Pt–C(3)	36.9(5)
C(1)–S–Pt	101.8(5)	C(5)–S–Pt	107.9(5)
C(5)–S–C(1)	103.0(7)	C(2)–C(1)–S	106.7(9)
C(3)–C(2)–C(1)	112.8(12)	C(2)–C(3)–Pt	107.2(9)
C(4)–C(3)–Pt	69.8(7)	C(4)–C(3)–C(2)	123.5(14)
C(3)–C(4)–Pt	73.2(7)	C(6)–C(5)–S	110.5(9)
C(7)–C(6)–C(5)	116.1(14)	C(8)–C(7)–C(6)	134.3(29)

Table 2. Characterisation of the complexes

Complex	Nature	M.p./°C	Analysis/%: C		H	
$[PtCl_2L^1]$	Yellow crystals	104	22.10	(23.55)	3.15	(3.45)
$[PtBr_2L^1]$	Dark yellow crystals	122	19.40	(19.35)	2.85	(2.85)
$[PtI_2L^1]$	Orange crystals	104	16.50	(16.25)	2.30	(2.40)
$[PtCl_2L^5_2]$	Yellow crystals	126	24.85	(24.90)	5.00	(5.15)
$[PtCl_2L^4]$	Yellow crystals	130—131	30.20	(31.05)	4.65	(4.80)
$[PtCl_2L^2]$	Yellow needles	138	21.05	(21.10)	3.15	(3.10)
$[PtBr_2L^2]$	Yellow crystals	112	17.65	(17.65)	2.55	(2.60)
$[PtI_2L^2]$	Orange crystals	91	15.10	(15.05)	2.15	(2.20)
$[PdCl_2L^5_2]$	Pale orange crystals	108—109	40.60	(41.65)	6.00	(6.10)
$[PtCl_2L^6]$	Light yellow crystals	152	27.70	(27.55)	4.05	(4.15)
$[PtBr_2L^6]$	Yellow crystals	146	23.05	(22.85)	3.45	(3.45)
$[PtI_2L^6]$	Orange crystals	108	19.30	(19.40)	2.90	(2.95)

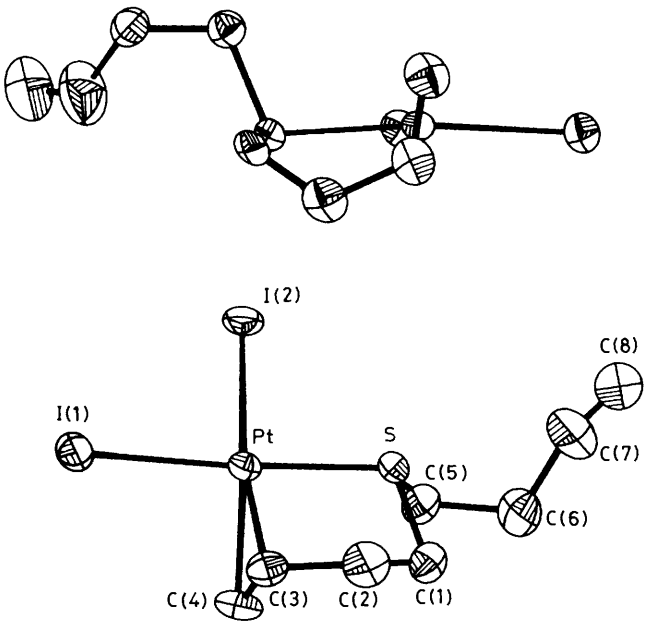

Figure 1. Two views of the crystal structure of *cis*-di-iodo(5-thianona-1,8-diene)platinum(II) showing the pseudo-axial orientation at S of the pendant alkenyl chain

Table 4. Fractional atomic co-ordinates ($\times 10^4$) for $[PtI_2L^1]$

Atom	*x*	*y*	*z*
Pt	969.2(3)	1 290.7(4)	1 859.4(3)
I(1)	400.8(6)	2 794.6(10)	909.2(7)
I(2)	546.3(7)	3 594.9(8)	4 070.3(8)
S	1 290(2)	−47(3)	4 566(2)
C(1)	1 468(9)	−1 973(11)	4 049(11)
C(2)	731(12)	−2 153(14)	2 902(12)
C(3)	895(12)	−965(13)	1 994(12)
C(4)	1 840(11)	−277(15)	1 979(11)
C(5)	2 577(9)	465(13)	5 349(11)
C(6)	2 867(11)	−479(19)	6 473(12)
C(7)	2 110(20)	−447(31)	7 291(20)
C(8)	2 155(20)	−45(26)	8 291(20)

N.m.r. Studies.—Variable-temperature ^1H n.m.r. data for the complexes are reported in Table 5. It is reasonable to assume that in the solid state each of the complexes has a similar structure to that of $[PtI_2L^1]$ discussed above. In solution however the n.m.r. spectra are consistent with the presence of two species for each complex, as discussed in detail below.

At very low temperatures (−90 °C) the ^1H n.m.r. spectra for the metal complexes of L^1 and L^2 indicate the presence of two alkene moieties in different environments: one co-ordinated (^1H resonances at δ 4.1, 4.5, and 5.0) and one unco-ordinated (resonances at δ 5.1 and 5.75). Conclusive proof for this would be the retention of $^2J(^{195}Pt-^1H)$ coupling between the metal atom and the alkene protons of the co-ordinated alkene moiety. Attempts to resolve the ^{195}Pt satellites, however, are thwarted by the short τ_1 values at low temperatures which result from the temperature dependence of the chemical shift anisotropy (c.s.a.) term in the expression for the platinum nucleus relaxation.[11] This results in satellite lines which are too broad to observe. This postulate is supported by a comparison with the low-temperature spectrum of the related complex *cis*-di-iodo(6-thiahex-1-ene)platinum(II)[3] where there is a single, static, bound alkene and the ^{195}Pt satellites are again unresolved.

The i.r. spectra of the L^1 and L^2 complexes in the solid state

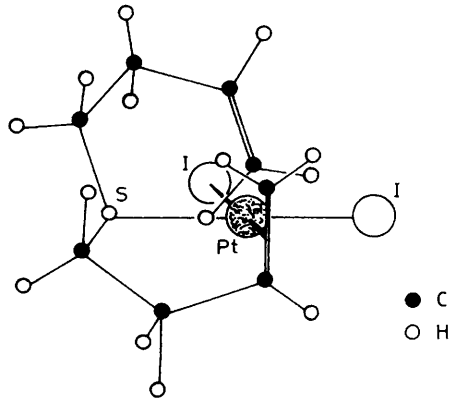

Figure 2. Drawing to illustrate the idealised geometry of $[PtI_2L^1]$ at the closest approach of the pendant alkene to the site of the co-ordinated alkene. The pendant chain is shown oriented pseudo-axially at S, as was observed in the solid state

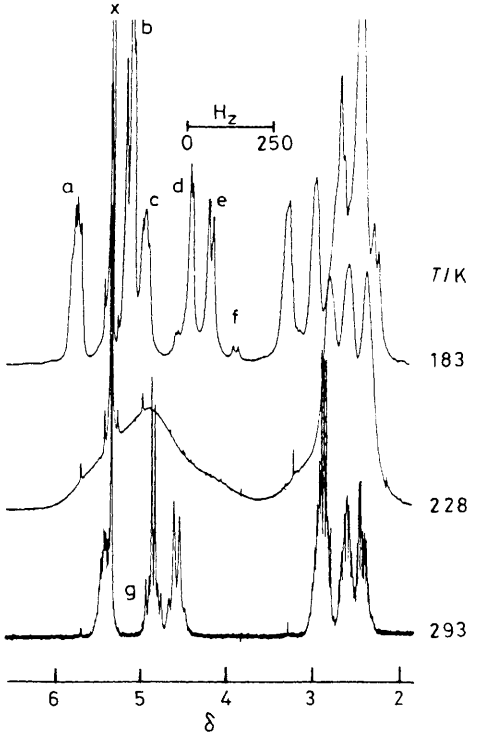

Figure 3. Variable-temperature ^1H n.m.r. spectra of $[PtCl_2L^2]$ showing the essentially static state spectrum at 183 K, the spectrum during coalescence at 228 K, and the spectrum at fast alkene exchange at 293 K. Peaks: a = unco-ordinated R^1, b = unco-ordinated R^2, R^3, c = co-ordinated R^1, d = co-ordinated R^2, e = co-ordinated R^3, f = minor isomer peaks, g = ^{195}Pt satellites, $^2J(^{195}Pt-^1H) = 34$ (exchanging); *c.f.* $[PtCl_2(MeSeCH_2CH_2CH{=}CH_2)]$, $^2J(^{195}Pt-^1H) = 64$(static), and x = solvent (CD_2Cl_2) = 68 Hz (static), and x = solvent (CD_2Cl_2)

are consistent with the low-temperature n.m.r. data in that each shows two bands at approximately 1 500 and 1 640 cm^{-1} (see Table 1). These are characteristic of co-ordinated and unco-ordinated alkene respectively.

At low temperatures the presence of second sets of co-ordinated alkene proton resonances indicates the existence of two epimers due to the two possible configurations at the chalcogen atom (pseudo-axial or pseudo-equatorial α-carbon atom in the pendant chain). At −90 °C the epimers exist in the ratio 1.5 : 1 for $[PtCl_2L^1]$, that in greater abundance being assumed to be the pseudo-axial epimer which allows the very close approach of the pendant alkene to the bound alkene,

Table 5. Variable temperature ^1H n.m.r. data for the alkene substituents in the static state, and at fast exchange. All values refer to alkenic protons ($R^1 = R^2 = R^3 = H$), except where indicated. Solvent is $CDCl_3$ except where indicated

	Values at static state (low temperature)					
	$\delta(R^1)$		$\delta(R^2)$		$\delta(R^3)$	
Sample	Co-ordinated	Unco-ordinated	Co-ordinated	Unco-ordinated	Co-ordinated	Unco-ordinated
L^1	—	5.82	—	5.05	—	5.05
L^3	—	5.79	—	5.00	—	5.00
L^5	—	—	—	4.83	—	4.83
$L^{4\,a}$	—	5.15	—	1.62	—	1.70
$L^{6\,b}$	—	1.75	—	4.78	—	4.74
L^2	—	5.84	—	5.05	—	5.05
$[PtCl_2L^1]^{c,d}$	4.95	5.74	4.54[e]	5.12	4.08[e]	5.12
$[PtBr_2L^1]^c$	5.09[f]	5.72	4.89	5.12	4.16	5.12
$[PtI_2L^1]^c$	4.95[f]	5.72	*g*	5.12	4.18	5.12
$[PtCl_2L^5]$	—	—	—	5.15	—	5.15
$[PtCl_2L^4]^a$	4.75	5.08	1.83	1.62	1.74	1.70
$[PtCl_2L^6]^{b,c}$	1.95	1.67	4.45	4.76	4.05	4.76
$[PtBr_2L^6]^{b,c}$	1.96	1.67	4.10	4.76	3.55[g]	4.76
$[PtI_2L^6]^{b,c}$	1.98	1.68	4.75	5.22	4.16	5.22
$[PtCl_2L^2]^c$	4.92	5.75	4.41	5.13	4.18	5.13
$[PtBr_2L^2]^c$	4.75[f]	5.71	4.60	5.08	4.16	5.08
$[PtI_2L^2]^c$	*g*	*g*	*g*	*g*	*g*	*g*
$[PdCl_2L^5]$	—	—	—	5.08	—	5.08

	Values at fast alkene exchange					
$\delta(R^1)$	$\delta(R^2)$	$\delta(R^3)$	$^2J(R^1\text{–}R^2)$	$^2J(R^1\text{–}R^3)$	$^3J(Pt\text{–}R^2)$	$^3J(Pt\text{–}R^3)$
—	—	—	—	—	—	—
—	—	—	—	—	—	—
—	—	—	—	—	—	—
—	—	—	—	—	—	—
—	—	—	—	—	—	—
—	—	—	—	—	—	—
5.43	4.91	4.62	9.5	16.0	34.0	32.0
5.50	5.06	4.68	9.2	15.1	33.0	31.0
5.52	5.23	4.75	9.9	15.8	34.9	31.0
—	—	—	—	—	—	—
h	*h*	*h*	*h*	*h*	*h*	*h*
1.95	4.80	4.44	—	—	34.3	35.6
1.94	4.91	4.47	—	—	35.4	35.7
1.95	5.17	4.52	—	—	34.8	35.0
5.42[i]	4.91	4.58	9.3	15.0	34.0	30.0
5.46	5.00	4.63	9.3	15.5	35.0	31.0
5.54	5.20	4.66	8.6	15.1	36.0	30.2
—	—	—	—	—	—	—

[a] $R^2 = R^3 = Me$. [b] $R^1 = Me$. [c] Solvent: dichloromethane at low temperature. [d] Solvent: dichloromethane. [e] Average of epimer values. [f] Approximate value only as signals overlapped. [g] Not resolved at −90 °C. [h] Fast-exchange temperature too high.

facilitating replacement (see Figure 2). This is also consistent with the *X*-ray structure analysis of $[PtI_2L^1]$ discussed above in which the pendant alkenyl chain adopted a pseudo-axial orientation.

As the temperature is raised, the alkene signals in the ^1H n.m.r. spectrum undergo a broadening and gradual coalescence as the co-ordinated alkene begins to exchange with the un-co-ordinated alkene (see Figure 3). At about −50 °C the coalescence temperature, T_c, is reached and the lines are very broad. Raising the temperature further results in the gradual sharpening of the lines until, at around 20 °C (for $[PtCl_2L^1]$), the alkene replacement becomes fast on the n.m.r. time-scale, resulting in an average alkene environment. This is reflected in the chemical shifts and coupling constants of the alkene protons which are the average of those for free and bound alkene protons. For example, in the case of $[PtCl_2L^1]$ the chemical shifts of the alkene protons R^1, R^2, and R^3 at room temperature are midway between those observed at low temperature for the protons of the co-ordinated and unco-ordinated alkenes (see Table 5) which is consistent with co-ordination of each alkene for one half of the time. This is further confirmed by examination of the $^2J(^{195}Pt\text{–}^1H)$ coupling constants for the alkene protons. In the case of $[PtCl_2L^1]$ at 20 °C, the values for the terminal alkene protons R^2 and R^3 in L^1 are 33 and 35 Hz respectively. As discussed above these coupling constants cannot be determined for the protons of the co-ordinated alkene in the static structure at low temperature. In the closely related complex $[PtCl_2(MeSCH_2CH_2CH{=}CH_2)]$,[3] however, where there is no possibility of alkene replacement, the corresponding terminal alkene protons have $^2J(^{195}Pt\text{–}^1H)$ values of 66 and 70 Hz respectively.

The different chalcogen epimers do not give rise to different resonances at room temperature because the alkene-replacement process effectively destroys much of the steric difference between the two alkene groups. At the low temperatures, in the static case, the steric differences are more pronounced and thus more evident.

In our previous study on potentially chelating sulphur–

Table 6. Coalescence and energy barrier data from variable-temperature ^{1}H n.m.r. studies

Complex	T_c ($S_{inv.}$)/K	Protons coalescing at T_c ($S_{inv.}$)	$\Delta G^{\ddagger}[T_c(S_{inv.})]$/kJ mol^{-1}	T_c (olefin exchange)/K	Protons coalescing at T_c (olefin exchange)	$\Delta G^{\ddagger}$ [T_c (olefin exchange)]/kJ mol^{-1}
[$PtCl_2L^1$]	370	SCH_2	76.6	231[a]	R^2, R^3	45.9[a]
[$PtBr_2L^1$]	353	SCH_2	75.5	223	R^3	42.3
[PtI_2L^1]	343	SCH_2	70.8	210	R^3	39.9
[$PtCl_2L^2$]	450[b]	SCH_2	95[b]	228[a]	R^2, R^3	43.9[a]
[$PtBr_2L^2$]	*c*	—	—	208	R^3	39.5
[PtI_2L^2]	*c*	—	—	193	R^3	36.7
[$PtCl_2L^6$]	373	SCH_2CH_2	79.9	225	R^3	52.02
[$PtBr_2L^6$]	373	SCH_2	80.4	213	R^3	43.8
[PtI_2L^6]	363	SCH_2	76.9	233	R^3	49.6
[$PtCl_2L^4$]	358	SCH_2	73.4	*d*	*d*	72.1[d]
[$PtCl_2L_2^5$]	280	SCH_2	56.9	—	—	—
[$PtCl_2L_2^5$]	243	SCH_2	49.8	—	—	—

[a] Average of epimer values. [b] Estimated. [c] Too high to be observed. [d] At 298 K. From two-dimensional EXSY n.m.r. and by bandshape analysis; $\Delta H^{\ddagger}_{298} = 55 \pm 4$ kJ mol^{-1}, $\Delta S^{\ddagger}_{298} = -57 \pm 13$ J K^{-1} mol^{-1}.

alkene ligands[3] where, however, there was only one alkene moiety, the energy barriers to sulphur inversion at the coalescence temperatures for the ligands containing the same alkenyl moiety were found to about 4 kJ mol^{-1} higher than those in the present case. A possible explanation for this is that the alkene rotation process for the dialkenyl chalcogenide complexes allows the sulphur atom to undergo inversion more easily as the alkene ligands replace each other, when presumably there is less steric strain within the ring system, than when no such strain-alleviating process can occur. The nature of the chalcogen atom (whether sulphur or selenium) does not significantly affect the energy barriers to alkene replacement in the complexes, but it has considerable effect on the energy barrier to configurational inversion of the chalcogen atom, and for the selenide complexes the coalescence temperature is increased to a point too high to be measured. Based on inversion data for other sulphide and selenide complexes of platinum(II),[12] an estimate of the energy barrier for selenium inversion as being about 20 kJ mol^{-1} greater than the barrier for sulphur inversion gives the estimated coalescence temperature as approximately 175 °C, indeed too high for n.m.r. analysis in solution. The coalescence data for the sulphur-inversion and alkene-replacement processes are summarised in Table 6.

The complex nature of the proton spin system in ligands such as L^1, and L^2, precluded a more detailed analysis of the variable-temperature ^{1}H n.m.r. data. It was therefore decided to design a ligand which would be amenable to such a study. The ligand chosen was L^4, in which the terminal alkene protons were replaced by methyl groups. These methyl groups gave ^{1}H n.m.r. signals in an otherwise clear region of the spectrum.

It was possible for this complex alone quantitatively to evaluate the rate constants for the alkene-exchange process at a series of temperatures. At temperatures between 10 and 40 °C, where the alkene replacement is relatively slow, it was decided to use two-dimensional n.m.r. exchange spectroscopy (EXSY),[13] a method pioneered in this department. The method has the advantage of being applicable to very slow rates of exchange. It also enabled us clearly to assign exchanging pairs of methyl resonances. Figure 4 shows an example of a two-dimensional phase-sensitive spectrum obtained using the Bruker automation program NOESYPH. Mixing times for these experiments were in the range 0.1—1 s. The F_1 data table contained 64 words zero-filled to 256 words, while the F_2 domain contained 256 words, and was not zero-filled. Data were Fourier transformed using an exponential window with line broadening of 1 Hz in both dimensions. Rate constants were

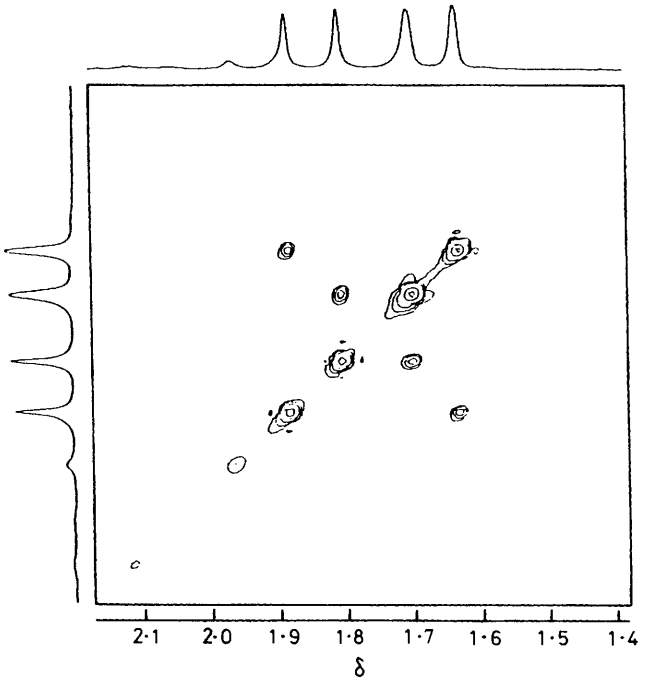

Figure 4. Two-dimensional ^{1}H n.m.r. spectrum of [$PtCl_2L^4$] (methyl region) at 20 °C with mixing time $\tau_m = 0.2$ s. Rate constants obtained by matrix analysis of cross-peak intensities. The cross-peaks clearly identify the exchanging co-ordinated and unco-ordinated methyl groups

calculated from signal intensities using the computer program D2DNMR.[13]

At 60 °C, where considerable line broadening occurs, the rate constant was obtained by complete bandshape analysis which involves the visual fitting of a computer-generated spectrum with that obtained experimentally according to the modified method of Kleier and Binsch[14,15] (see Figure 5). The somewhat drastic effects of the methyl substituents on the energy barrier to olefin replacement are reflected in the increase in coalescence temperature for this process from −50 °C for [$PtCl_2L^1$] to approximately +100 °C for [$PtCl_2L^4$] and the concomitant increase in $\Delta G^{\ddagger}$ from 46.0 to 72.1 kJ mol^{-1}; $\Delta H^{\ddagger}$ was found to be 55 ± 4 kJ mol^{-1} and $\Delta S^{\ddagger}$ was evaluated as −57 ± 13 J K^{-1} mol^{-1} (see Figure 6). The methyl substituents have a steric and an electronic effect, both of which reduce the ease of olefin replacement in the complex. Sterically, the methyl groups

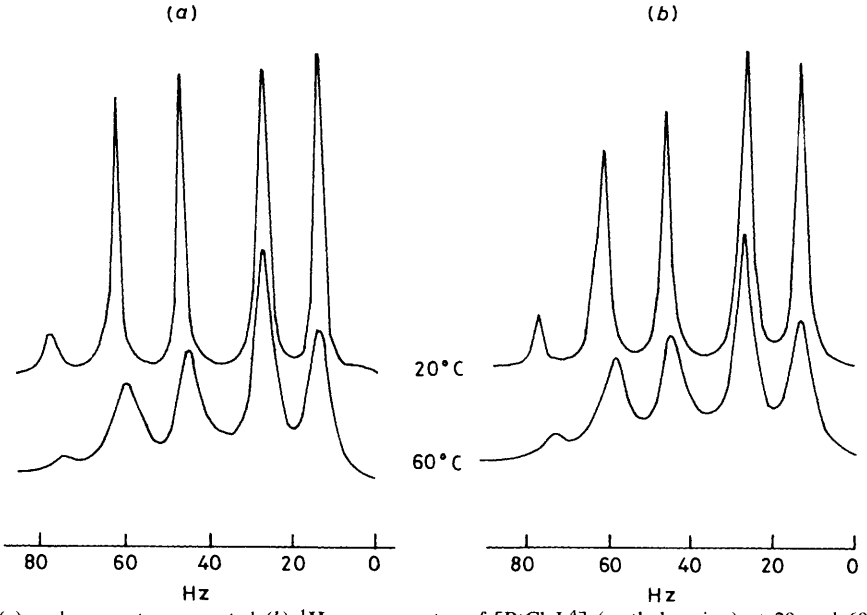

Figure 5. Experimental (*a*) and computer-generated (*b*) ^{1}H n.m.r. spectra of $[PtCl_2L^4]$ (methyl region) at 20 and 60 °C used in the complete bandshape analysis to find the rate constant for the alkene-exchange process at 60 °C

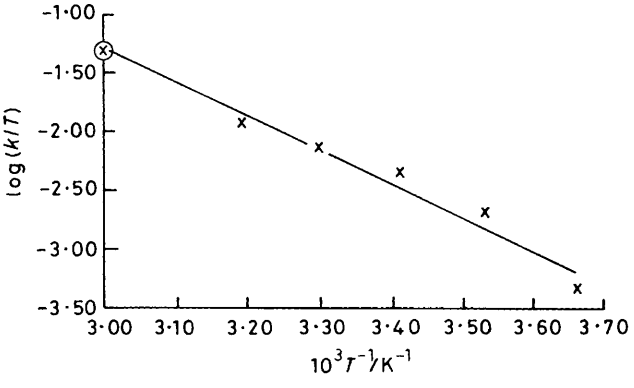

Figure 6. Eyring plot of log (k/T) *vs.* 10^3 T^{-1} to give $\Delta G_\theta^\ddagger$, $\Delta H_\theta^\ddagger$, and $\Delta S_\theta^\ddagger$ for $[PtCl_2L^4]$. Points marked 'X' obtained from cross-peak intensities in the two-dimensional ^{1}H n.m.r. spectra; point marked '⊗' obtained by complete bandshape analysis

hinder the approach of the pendant olefin to the co-ordinated olefin. Electronically, the methyl substituents cause an increase in the energy barrier to labilisation of the co-ordinated olefin moiety by the release of electron density from the methyl groups into the double bond and the consequent increase in the donation of electron density from the double bond to the metal (in a σ bond) which results in a stronger olefin–metal bond.

The nature of the halogen is also a determining factor in the values of the energy barriers to the transition states for both fluxional processes. It is apparent that the energy barriers decrease as the halogen is changed in the order Cl > Br > I. This is due to the *trans* influence of the halogen: the larger more polarisable iodide ion exerts a stronger *trans* influence than does the bromide or chloride ion, resulting in the olefin being less strongly bound to the metal, due to a reduction in the π-back bonding, and the electrons in the M–S bond being drawn more towards the metal. These effects are manifested as reductions in the energy barriers to the fluxional processes.

Experimental

Reactions were carried out using standard Schlenk techniques under nitrogen (although the products are not noticeably air- or water-sensitive) and solvents were dried and distilled under nitrogen before use.

The dialkenyl sulphide ligands were prepared from the alkenyl bromide (2 equivalents) and sodium sulphide in a two-phase liquid system using tributylhexadecylphosphonium bromide as a phase-transfer catalyst,[16] and distilled under vacuum. The selenide ligand 5-selenanona-1,8-diene was prepared by the reaction of sodium selenide (formed *in situ*) with the alkenyl bromide: to a stirred solution of sodium hydroxide (16.21 g, 405.2 mmol) in water (70 cm^3) at 50 °C was added Rongalit (sodium hydroxymethanesulphinate) (25.00 g, 162.2 mmol) and selenium powder (5.852 g, 74.1 mmol). To this was added dropwise 4-bromobut-1-ene (10.00 g, 74.1 mmol) and the mixture was refluxed at 100 °C for 6 h. After diethyl ether extraction of the cool mixture, drying over magnesium sulphate, and distillation at 48 °C (1 mmHg, 133 Pa), the ligand was obtained as a very pale yellow liquid (4.40 g, 31%).

Preparation of the complexes *cis*-$[MX_2(L)]$ (X = Cl, Br, or I; M = Pd or Pt; L = dialkenyl chalcogenide ligand) is exemplified below by that of $[PtCl_2L^1]$.

Preparation of cis-*Dichloro*(5-*thianona*-1,8-*diene*)*platinum*(II), $[PtCl_2L^1]$.—To a stirred solution of potassium tetrachloroplatinate(II) (1.00 g, 2.41 mmol) in water (10 cm^3), ethanol (3 cm^3), and 1 mol dm^{-3} hydrochloric acid (0.5 cm^3) was added 1 equivalent of the dialkenyl chalcogenide ligand, L^1 (0.342 g, 2.41 mmol) in ethanol (2 cm^3). The initially red solution was left to stir at room temperature overnight. After washing the resulting pale yellow precipitate with water, ethanol, and ether and drying *in vacuo*, the product was obtained as a powder in high yield (0.84 g, 91%). The product may be crystallised from warm chloroform or a chloroform–hexane two-layer liquid system.

Preparation of Bromo- and Iodo-derivatives.—These were prepared by metathesis of the chloro-derivative in warm acetone solution using the appropriate lithium halide in excess.

For example, to prepare *cis*-di-iodo(5-thianona-1,8-diene)-

Table 7. Crystal data, details of intensity measurements, and structure refinement for $[PtI_2L^1]$

Formula	$C_8H_{14}I_2PtS$
M	591.158
Crystal system	Monoclinic
Space group	$P2_1/n$
a/Å	13.249(3)
b/Å	8.804(3)
c/Å	11.656(3)
U/Å^3	1 334.0(6)
β/°	101.05(2)
Z	4
D_c/g cm^{-3}	2.943
$F(000)$	1 048
Crystal size (mm)	0.87 × 0.62 × 0.13
μ(Mo-K_α)/cm^{-1}	153.2

platinum(II), a solution of lithium iodide (0.578 g, 4.315 mmol) in acetone (5 cm^3) was added to a warm (50 °C) stirring solution of *cis*-dichloro(5-thianona-1,8-diene)platinum(II) (0.503 g, 1.233 mmol) in acetone (30 cm^3). The colour darkened as the iodo-derivative formed. The solution was filtered, the acetone removed under reduced pressure, and the product recrystallised from chloroform after filtration again to remove lithium chloride.

N.M.R. Studies.—Proton n.m.r. experiments were performed on a Bruker AM250 instrument at 250 MHz. Low-temperature spectra (−90 to −20 °C) were taken in CD_2Cl_2; for temperatures in the range −30 to +55 °C, $CDCl_3$ was used, and above 55 °C, 1,1,2,2-tetrachloroethane was used.

Single-crystal X-Ray Crystallographic Structural Determination of $[PtI_2L^1]$.—Crystals of $[PtI_2L^1]$ suitable for *X*-ray analysis were grown from a chloroform solution, induced to crystallise by the addition of a layer of hexane. The crystal data, details of intensity measurements, and structure refinement are summarised in Table 7.

Data collection. Unit-cell parameters and intensity data were obtained by following previously detailed procedures,[17] using a CAD4 diffractometer operating in the ω–2θ scan mode, with graphite monochromated Mo-K_α radiation. A total of 2 641 unique reflections were collected ($3 < 2\theta < 50°$). The segment of reciprocal space scanned was (h) −15 to 15, (k) 0 to 10, (l) 0 to 13. The reflection intensities were corrected for absorption using the azimuthal-scan method;[18] maximum transmission factor 1.00, minimum value 0.39.

Structure solution and refinement. The structure was solved by the application of routine heavy-atom methods (SHELX 86),[19] and refined by full-matrix least squares (SHELX 76).[20] After isotropic refinement of all non-hydrogen atoms, the DIFABS method of absorption correction[21] was applied (maximum transmission factor 1.176, minimum value 0.726). Refinement was continued with anisotropic thermal parameters for all non-hydrogen atoms. Only methylene hydrogen atoms were included in the model and these were placed in calculated positions (C–H 0.96 Å, $U = 0.10$ Å^2). The final residuals R and R' were 0.040 and 0.044 respectively for the 109 variables and 1 996 data for which $F_o \geqslant 6\sigma(F_o)$. The function minimised was $\Sigma w(|F_o| - |F_c|)^2$ with the weight, $w = 1/[\sigma^2(F_o) + 0.0003F_o^2]$.

Atomic scattering factors and anomalous scattering parameters were taken from refs. 22 and 23 respectively. All computations were made on a DEC VAX-11/750 computer.

Additional material available from the Cambridge Crystallographic Data Centre comprises H-atom co-ordinates and thermal parameters.

References

1 D. C. Goodall, *J. Chem. Soc. A*, 1968, 887.
2 R. McCrindle, E. C. Alyea, G. Ferguson, S. A. Dias, A. J. McAlees, and M. Parvez, *J. Chem. Soc., Dalton Trans.*, 1980, 137.
3 E. W. Abel, P. A. Bates, D. G. Evans, M. Hursthouse, J. R. Koe, and V. Sik, *J. Chem. Soc., Dalton Trans.*, 1989, 985.
4 M. A. Bennett, H. W. Kouwenhoven, J. Lewis, and R. S. Nyholm, *J. Chem. Soc.*, 1964, 4570.
5 P. W. Clark and G. E. Hartwell, *Inorg. Chem.*, 1970, **9**, 1948.
6 E. W. Abel, R. P. Bush, F. J. Hopton, and C. R. Jenkins, *Chem. Commun.*, 1966, 58.
7 P. Haake and P. C. Turley, *J. Am. Chem. Soc.*, 1967, **89**, 4611.
8 J. A. Wunderlich and D. P. Mellor, *Acta Crystallogr.*, 1954, **7**, 130; 1955, **8**, 57.
9 P. R. H. Alderman, P. G. Owston, and J. M. Rowe, *Acta Crystallogr.*, 1960, **13**, 149.
10 H. C. Freeman and M. L. Golumb, *Chem. Commun.*, 1970, 1523.
11 P. S. Pregosin, *Annu. Rep. NMR Spectrosc.*, 1986, **17**, 285.
12 E. W. Abel, S. K. Bhargava, K. Kite, K. G. Orrell, V. Sik, and B. L. Williams, *Polyhedron*, 1982, **1**, 289.
13 E. W. Abel, T. P. J. Coston, K. G. Orrell, V. Sik, and D. Stephenson, *J. Magn. Reson.*, 1986, **70**, 34.
14 D. A. Kleier and G. Binsch, *J. Magn. Reson.*, 1970, **3**, 146.
15 D. A. Kleier and G. Binsch, DNMR3 program 165, Quantum Chemistry Program Exchange, Indiana University, 1970.
16 D. Landini and F. Rolla, *Synthesis*, 1974, 565.
17 M. B. Hursthouse, R. A. Jones, K. M. A. Malik, and G. Wilkinson, *J. Am. Chem. Soc.*, 1979, **101**, 4128.
18 A. C. T. North, D. C. Phillips, and F. S. Mathews, *Acta Crystallogr., Sect. A*, 1968, **24**, 351.
19 G. M. Sheldrick, SHELX 86 Program for Crystal Structure Solution, University of Göttingen, 1986.
20 G. M. Sheldrick, SHELX 76 Program for Crystal Structure Determination and Refinement, University of Cambridge, 1976.
21 N. Walker and D. Stuart, *Acta Crystallogr., Sect. A*, 1983, **39**, 158.
22 D. T. Cromer and J. B. Mann, *Acta Crystallogr., Sect. A*, 1968, **24**, 321.
23 D. T. Cromer and D. Liberman, *J. Chem. Phys.*, 1970, **53**, 1891.

Received 26*th October* 1988; *Paper* 8/04265I